LIMNOLOGY and OCEANOGRAPHY

Taxon-specific dark survival of diatoms and flagellates affects Arctic phytoplankton composition during the polar night and early spring

Willem H. van de Poll,[1]* Edwin Abdullah,[1] Ronald J. W. Visser,[1] Philipp Fischer,[2] Anita G. J. Buma[1]
[1]Department of Ocean Ecosystems, Energy and Sustainability Research Institute Groningen, University of Groningen, Groningen, The Netherlands
[2]Biosciences, Shelf Sea System Ecology, Alfred Wegener Institute, Helgoland, Germany

Abstract

Effects of prolonged darkness on Arctic phytoplankton composition were investigated with lab experiments and a pigment time series in Kongsfjorden, Spitsbergen (78°55′N). Chlorophyll *a* (Chl *a*), pigment composition, particulate organic carbon, cell numbers, and photosynthetic characteristics were studied in Arctic diatoms (*Thalassiosira antarctica*, *Thalassiosira nordenskioeldii*) and flagellates (*Rhodomonas* sp., *Micromonas* sp.) during 8 weeks of darkness and subsequent recovery in irradiance. Loss of photosynthetic functionality after 2 weeks of darkness was reversible in all species when returned to irradiance. Diatoms were more resistant to prolonged darkness (> 2 weeks) compared to the flagellates, with lower decline rates of Chl *a* and maximum quantum yield of PSII. *T. nordenskioeldii* showed rapid growth during recovery throughout 8 weeks of dark incubation, whereas recovery of flagellates diminished within 4 weeks. Ratios of taxonomic marker pigments relative to Chl *a* of all species showed limited variation during 8 weeks of dark incubation. The experimentally observed enhanced dark survival of diatoms was in agreement with pigment observations during four polar nights (2013–2017) in Kongsfjorden, which showed increased relative diatom abundance during declining biomass (down to 0.02 mg Chl *a* m^{-3}). Therefore, a period of prolonged darkness gives Arctic diatoms a head start during the early stages of the spring bloom. The taxon-specific survival traits can influence the geographical distribution of diatoms and flagellates within the polar oceans and their phenology. Furthermore, the persistence of Chl *a* of nonviable phytoplankton during darkness might influence biomass estimates during the polar night.

Phytoplankton experiences strong fluctuations in irradiance exposure. These fluctuations are most pronounced at latitudes within the polar circles, where irradiance is modulated by extreme seasonal changes in solar elevation and sea ice cover, in addition to vertical mixing of the ocean (McMinn and Martin 2013). The period without photosynthetically available radiation (PAR) can extend to several months in the high Arctic. Phytoplankton responses to this phenomenon are relatively unknown due to inaccessibility of high latitude oceans during winter (Berge et al. 2015). High latitude spring bloom phytoplankton composition appears to follow a well-established pattern. Typically, diatoms and haptophytes are abundant in early spring when nutrient concentrations are high after winter regeneration and mixing, and irradiance experienced by phytoplankton increases (Wassmann et al. 1999). Considerable variability in phytoplankton survival

during darkness has been observed. Experimental work has shown that resting stages of diatoms and dinoflagellates survived for 27-112 months in sediment samples (Lewis et al. 1999). Vegetative stages of temperate benthic diatoms survived 1 yr of darkness, which coincided with an exponential decline in photosynthetic pigments (Veuger and van Oevelen 2011). The Arctic benthic diatom *Navicula* cf. *perminuta* used stored lipids, carbohydrates, and proteins as energy sources during 8 weeks of darkness, whereas phospho- and glycolipids of photosynthetic membranes remained unchanged (Schaub et al. 2017). On a shorter time scale the diatom *Thalassiosira weissflogii* reduced metabolic rate and cell division, whereas effects on Chlorophyll *a* (Chl *a*) content and photosynthetic capacity were negligible during 12 d of darkness (Walter et al. 2017). The above suggests that diatoms are well suited to survive long periods of darkness (Peters and Thomas 1996; Reeves et al. 2011). However, dark survival of other photosynthetic phytoplankton groups is less investigated. The Antarctic haptophyte *Phaeocystis antarctica* showed an eightfold reduction in Chl *a* and a 50% reduction in maximum quantum yield of PSII over 2 months of darkness, whereas recovery of photosynthesis required 20 d of light exposure (Tang et al. 2009).

*Correspondence: w.h.van.de.poll@rug.nl

Moreover, the cryptophyte *Rhodomonas* sp. initially continued to grow, but cell numbers decreased after 12 d of darkness, coinciding with decreasing carbohydrate and Chl *a* content (70% and 50%, respectively, Walter et al. 2017). The survival of long periods of darkness presumably relies on taxon-specific traits such as energy storage and utilization. Other survival strategies have also been suggested for flagellates such as mixotrophy (McKie-Krisberg and Sanders 2014; McKie-Krisberg et al. 2014; Joli et al. 2017; Stoecker and Lavrentyev 2018). Field observations during the Arctic polar night have so far not provided a clear picture on how the absence of irradiance affects phytoplankton species composition and physiology. DNA and RNA of all major taxonomic groups have been detected during the polar night in fjords on the west coast of Spitsbergen, although the relative abundance of these groups remains unknown (Vader et al. 2014; Marquardt et al. 2016). Furthermore, phytoplankton assemblages ($\geq 20\ \mu m$) obtained from Kongsfjorden during the polar night showed rapid initiation of carbon fixation when exposed to irradiance (Kvernvik et al. 2018). Currently, a systematic study investigating the responses of Arctic diatoms and flagellates to prolonged darkness is lacking. We tested the hypothesis that diatoms survive longer periods of darkness than flagellates by investigating the photophysiological responses of two Arctic diatoms and two flagellates to 8 weeks of darkness. In addition, we analyzed 4 yr of phytoplankton pigment observations in a high Arctic fjord (Kongsfjorden, Spitsbergen) to assess the abundance of diatom and flagellates during the polar night. Furthermore, we discuss the potential of these observations as a driver for high latitude phytoplankton spring bloom composition.

Materials and methods

Cultivation and dark incubation

The centric Arctic diatoms (*Thalassiosira antarctica* var *borealis* CCMP 982, *Thalassiosira nordenskioeldii* CCMP 997) and flagellates (*Rhodomonas* sp. CCMP 2045, *Micromonas* sp. SCCAPK0024) were cultivated for 4 weeks in F2 enriched seawater (Guillard and Ryther 1962) prior to the dark incubations. The diatom cultures originated from the Oslo Fjord and the Norwegian Sea, whereas *Micromonas* sp. was isolated in Spitsbergen and *Rhodomonas* sp. in Baffin Bay. Consequently, all cultures originated from cold to cold temperate waters with strong seasonality in irradiance. Cultivation was done in 1-liter conical flasks (two replicates per species) at 4.5°C in a cryostat controlled water bath exposed to 20 μmol photons m^{-2} s^{-1} over a 16:8 h light:dark cycle. The cultures were diluted each week with F2-enriched seawater to prevent nutrient limitation. Prior to the dark incubation, cultures were supplemented with nutrients (F2 concentrations). Afterward, the conical flasks were wrapped with aluminum foil and placed in a dark box in a climate room maintained at 5°C. Cultures were swirled semi-daily to prevent formation of aggregates. Subsamples (100 mL) were obtained from each flask under dim light after 0, 1, 2, 4,

6, and 8 weeks of dark incubation. Irradiance during sampling (~ 10 min) was below 0.5 μmol photons m^{-2} s^{-1} (Licor LI 250). Subsamples were placed on ice in a dark box until processing (within 30 min). The subsamples were used to determine cell numbers, Chl *a* concentration, pigment composition, particulate organic carbon (POC), photosynthetic characteristics, and for recovery experiments during subsequent irradiance exposure. After 8 weeks of darkness, the cultures were returned to the original irradiance conditions and visually inspected for growth during another 4 weeks.

Recovery experiments

Subsamples (16 mL) were incubated in transparent glass vials that were placed in a cryostat cooled irradiance setup. Combinations of neutral density foils were used to create five irradiance levels (2, 5, 12, 20, and 40 μmol photons m^{-2} s^{-1}) provided continuously for 5 d. Afterward, subsamples were obtained for Chl *a*, cell counts, and photosynthetic characteristics (fast repetition rate fluorometry [FRRf]).

Chl *a* and pigment composition

Samples (5 mL) were vacuum-filtered (−20 kPa) on 25 mm GF/F, snap frozen in liquid nitrogen, and stored at −80°C. Filters were freeze-dried (48 h), and pigments were extracted by 90% acetone at 4°C in darkness (48 h) (van Leeuwe et al. 2006). Chl *a* was measured using a fluorimeter (10-AU-005-CE, Turner Designs, Sunnyvale, CA, U.S.A.) calibrated by a Chl *a* standard dilution series (Sigma) with a spectrophotometrically measured concentration. Full pigment composition was determined using high-performance liquid chromatography (HPLC). Sampling and extraction was as described above. Pigments were separated using a (Waters 2695 separation module), with a Zorbax Eclipse extra dense bonding C$_8$ 3.5 μm column (Agilent Technologies) (Van Heukelem and Thomas 2001). Peaks were identified by retention time and diode array spectroscopy (Waters 996 photodiode array detector) and quantified using standard dilutions (DHI LAB products) of Chl *a*, chlorophyll *b* (Chl *b*), chlorophyll c_2 (Chl c_2), neoxanthin, prasinoxanthin, alloxanthin, fucoxanthin, diadinoxanthin (dd), diatoxanthin (dt), violaxanthin, antheraxanthin, zeaxanthin, and β-carotene at 436 nm. The deepoxidation state (DES) of the diatom xanthophyll pigment cycle was calculated as dt/(dd + dt).

Cell numbers

Samples (2 mL) were fixed with Lugol (0.04% final concentration, v:v) and were counted using Sedgewick-Rafter (diatoms, *Rhodomonas* sp.) and improved Neubauer (*Micromonas* sp.) counting chambers and an Olympus light microscope after 0.5 h sedimentation.

Fast repetition rate fluorometry

Samples (3.5 mL) for PSII photophysiology were measured using a FastOcean and Act2 FRRf (Chelsea Technologies Group, West Molesey, UK). All samples were dark adapted for 30 min

on ice prior to analysis. We used a blue LED excitation source (450 nm) to provide single turnover acquisitions consisting of a saturation phase of 100 flashlets on a 2 μs pitch and a relaxation phase of 40 flashlets on a 60 μs pitch. Fluorescence transients (mean of 19–20 single turnover acquisitions) were fitted according to Kolber et al. (1998) using Act2Run software (Chelsea) to obtain the minimum fluorescence-derived Chl a concentration (Chl aF0 in μg L^{-1}); the maximum quantum yield of PSII (F_v/F_m): the proportion of absorbed light in PSII that is used for photochemistry; the absorption cross section of PSII at 450 nm (σ_{PSII}[450] in nm^2 PSII^{-1}): the physical cross-section of PSII that is used for photochemistry; reopening time of closed reaction center II (RCII) (τ_{ES} in μs); PSII connectivity (ρ): the efficiency of energy transfer from closed to open RCIIs; Stern–Volmer Normalized Stern-Volmer (NSV) non-photochemical quenching (NPQ) measured at 700 μmol photons m^{-2} s^{-1}: the thermal dissipation of excess energy.

Particulate organic carbon

POC samples were obtained after dark incubation and after 5 d recovery at 20 μmol photons m^{-2} s^{-1}. Duplicate samples (5 mL) for POC were filtered onto 13 mm precombusted (4 h, 600°C) GF/F (Whatman), snap frozen in liquid nitrogen, and stored at −80°C. Prior to analysis, filters were acidified under HCl (37%) fumes for 4 h, dried overnight at 60°C, and wrapped in tin capsules (Elemental Microanalysis). Analysis was performed on a cavity ring-down spectrometer (G2101-I, Picarro) with a combustion module (Costech).

Pigment monitoring Kongsfjorden (Spitsbergen)

Pigment samples were collected as part of a monitoring program at the Ferrybox site in Ny Ålesund, Spitsbergen (78°55′N, Underwater Observatory, Fischer et al. 2017; Van de Poll et al. 2016). Here, seawater is obtained from Kongsfjorden at 11 m depth in front of the old jetty. Weekly 10 L samples were collected at this site during four subsequent winters (October–March, 2013–2017) and filtered on 47 mm GF/F using mild overpressure (0.2 mbar). Filters were snap frozen in liquid nitrogen and stored and transported at −80°C. Extraction and analysis of pigments was done in the Netherlands as described above. Abundance of taxonomic groups was assessed using CHEMTAX (Mackey et al. 1996) as described in Van de Poll et al. (2016, 2018) using starting pigment ratios of diatoms, haptophytes, chrysophytes, prasinophytes, cryptophytes, and dinoflagellates.

Statistics

Trends (decline or increase rates week^{-1}) of photosynthetic characteristics and Chl a during dark incubation were determined using linear fits of each replicate ($n = 2$). Chl a decline rates of flagellates were calculated after the initial increase (week 1) to week 6 (*Micromonas* sp.) and week 8 (*Rhodomonas* sp.), whereas decline rates of diatoms were calculated during 8 weeks of dark incubation. Trends in photosynthetic characteristics were calculated from week 0 to 6 for the flagellates and

from week 0 to 8 for the diatoms. The trends of flagellates (*Micromonas* sp., *Rhodomonas* sp.) and diatoms (*T. antarctica*, *T. nordenskioeldii*) were pooled and tested for significance using a *t*-test or a rank sum test ($p < 0.05$). Changes in pigment ratios relative to Chl a during dark incubation were tested for significance using Spearman Rank order correlation. Trends in monthly averaged taxonomic composition and Chl a concentrations from October to March in Kongsfjorden were tested for significance using Spearman Rank order correlation.

Results

### Chl a, POC, and cell numbers during darkness

Chl a concentration of *Micromonas* sp. cultures increased during the first week of darkness and declined afterward, whereas *Rhodomonas* sp. Chl a was constant during the first 2 weeks and declined afterward (Fig. 1). *T. antarctica* and *T. nordenskioeldii* Chl a also showed a declining trend. Linear rates of Chl a decline were significantly faster for flagellates as compared to diatoms (-16.9 ± 1.6 week^{-1} vs. -5.4 ± 2.3 week^{-1}, respectively) ($p < 0.001$) (Table 1). HPLC determined and FRRf derived Chl a showed similar trends in linear decline rates (Table 1; Fig. 2). After 8 weeks of darkness, Chl a declined to on average 56% of the initial concentration for the flagellates, whereas this was 70% for the diatoms.

Cell numbers of *Micromonas* sp. and *Rhodomonas* sp. increased during the first 2 weeks of dark incubation and declined afterward, whereas diatom cell numbers showed no significant trend (Fig. 3). Pigmentation of *Micromonas* sp. decreased strongly after 2 weeks of darkness, reducing the reliability of cell counts for longer dark incubations. Cellular Chl a at the start of the experiment was on average 3.8 ± 0.5 pg, 5.3 ± 1.0 pg, 0.6 ± 0.3 pg, and 1.6 ± 0.8 pg per cell for *T. antarctica*, *T. nordenskioeldii*, *Micromonas* sp., and *Rhodomonas* sp., respectively. Cellular Chl a of *Rhodomonas* sp. showed a declining trend from week 4 to week 8 during dark incubation, whereas *Micromonas* sp. showed declining cellular Chl a during week 0–2, with an unclear trend afterward (results not shown). Trends in diatom cellular Chl a were not significant.

Rhodomonas sp. POC showed a declining trend (-7.2 μg carbon week^{-1}, Fig. 4, Table 1). POC concentrations of the other cultures showed no consistent trends during 8 weeks of dark incubation. Carbon:Chl a of *Micromonas* sp. increased 1.6-fold during week 4, 6, and 8 as compared with week 0, 1, and 2 (Table 2). Carbon:Chl a of the other species showed no significant trends during 8 weeks of dark incubation (Tables 2, 3).

Pigment composition during darkness

Chl a of *T. nordenskioeldii* and *T. antarctica* showed significant declining trends of -7 μg Chl a week^{-1} and -4 μg Chl a week^{-1}, respectively. Chl c_2 also showed declining trends (-0.8 and -0.5 μg week^{-1}). Fucoxanthin of *T. antarctica* remained unchanged relative to Chl a whereas this ratio showed a minor increase in *T. nordenskioeldii* (Table 2). The xanthophyll cycle
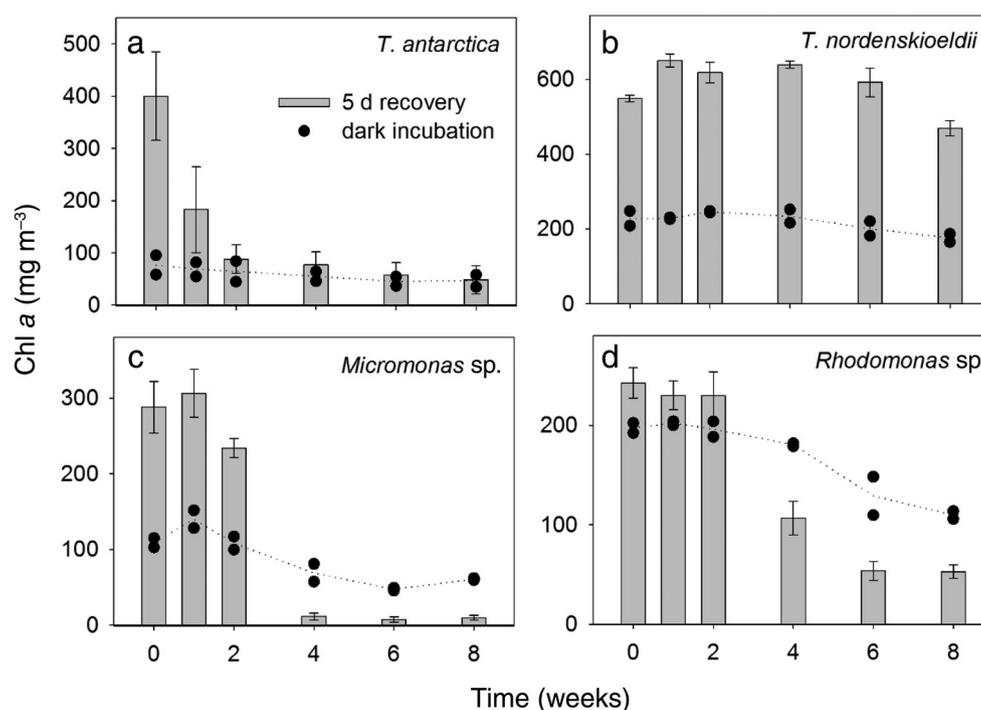
Fig. 1. Chl *a* during 8 weeks of dark incubation (black symbols, $n = 2$) and subsequent recovery of subsamples during 5 d of irradiance of (**a**) *T. antarctica*, (**b**) *T. nordenskioeldii*, (**c**) *Micromonas* sp., and (**d**) *Rhodomonas* sp. The gray bars show the mean Chl *a* after 5 d of recovery in an irradiance gradient (2–40 μmol photons m^{-2} s^{-1}, $n = 10$).

pigments diadino and diatoxanthin increased relative to Chl *a* (significant for *T. nordenskioeldii*). Meanwhile, the DES of the xanthophyll cycle of *T. nordenskioeldii* and *T. antarctica* increased from 0.16–0.24 to 0.36–0.43 during 8 weeks of dark incubation (Table 2). *Micromonas* sp. Chl *a*, Chl *b*, Mg DVP, neoxanthin, prasinoxanthin, and β-carotene concentrations

declined by on average 50% when comparing pooled data of week 0, 1, 2 and 4, 6, 8, respectively. Ratios of the light harvesting pigment Chl *b* relative to Chl *a* increased by ~ 20%, whereas neoxanthin decreased by 16% relative to Chl *a* after 4 weeks of dark incubation (Table 3). Violaxanthin and zeaxanthin increased during 8 weeks of dark incubation, resulting in a

Table 1. Mean rates of change (week^{-1}) derived from linear fits of measurements during 8 weeks of dark incubation of *T. antarctica*, *T. nordenskioeldii*, *Micromonas* sp., and *Rhodomonas* sp. for Chl *a* concentration (Chl *a*, μg L^{-1}, fluorometry); Chl *a* (HPLC): Chl *a* concentration derived from HPLC; Chl *a* (F0): FRRf derived Chl *a*; carbon concentrations (mg L^{-1}); F_v/F_m: maximum quantum yield of PSII; ρ: PSII connectivity, the efficiency of energy transfer from closed to open RCIIs; $\sigma_{PSII}(450)$: absorption cross-section of PSII at 450 nm (nm^2 PSII^{-1}); τ_{ES}: reopening of closed PSII reaction centers (μs); NPQ (NSV): Normalized Stern-Volmer non-photochemical quenching at 700 μmol photons m^{-2} s^{-1}; rates of change of *Micromonas* sp. and *Rhodomonas* sp. Chl *a* and Chl *a* (F0) were calculated after initial increase during week 1, 2 of dark incubation (data shown in Fig. 1). *p* values for significant rates of change are indicated in brackets.

| Species	*T. antarctica*	*T. nordenskioeldii*	*Micromonas* sp.	*Rhodomonas* sp.
Parameter				
Chl *a*	−3.9 (0.036)	−6.5 (0.009)	−18.2 (< 0.001)	−14.2 (< 0.001)
Chl *a* (HPLC)	−3.6 (0.043)	−6.8 (0.002)	−19.0 (< 0.001)	−14.8 (0.019)
Chl *a* (F0)	−2.2 (0.001)	−5.0 (< 0.001)	−23.4 (< 0.001)	−21.2 (< 0.001)
Carbon	ns	ns	ns	−7.20 (0.002)
F_v/F_m	−0.01 (0.003)	−0.02 (< 0.001)	−0.12 (< 0.001)	−0.07 (< 0.001)
ρ	ns	−0.03 (< 0.001)	−0.08 (0.015)	−0.06 (< 0.001)
$\sigma_{PSII}(450)$	−0.07 (< 0.001)	−0.08 (< 0.001)	−0.54 (0.002)	−0.27 (0.003)
τ_{ES}	490 (< 0.001)	591 (< 0.001)	2364 (0.004)	1359 (< 0.001)
NPQ (NSV)	0.03 (0.009)	0.08 (< 0.001)	0.28 (0.005)	0.49 (< 0.001)

ns, no significant trend.
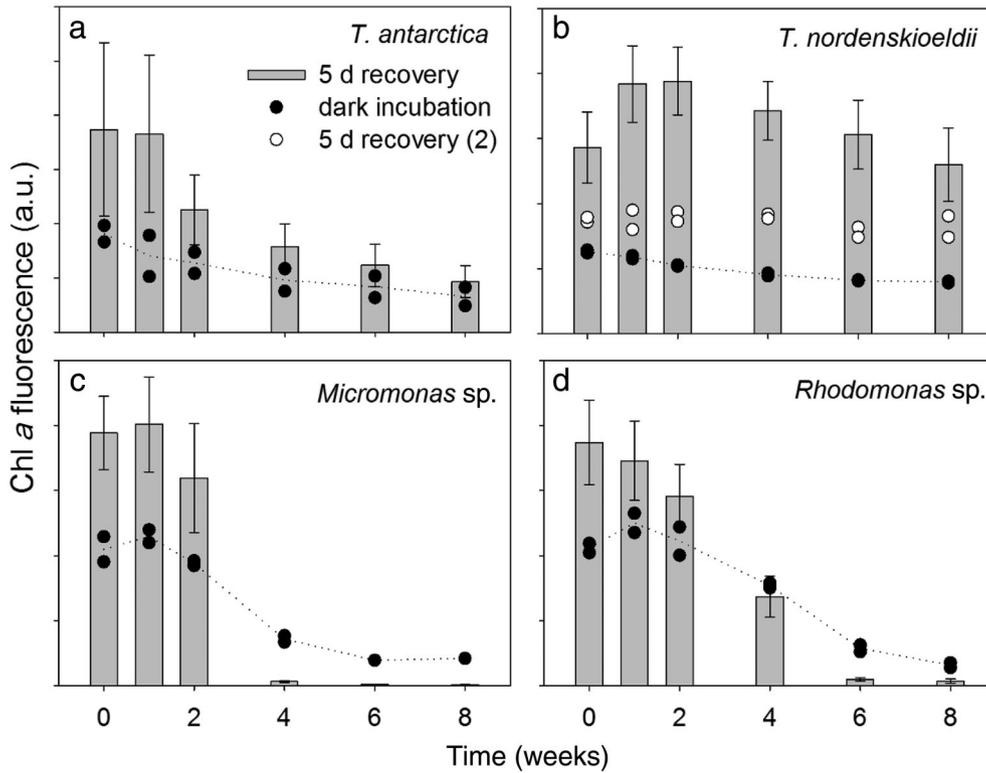
Fig. 2. Chl *a* fluorescence (FRRf) during 8 weeks of dark incubation (black symbols, *n* = 2) and subsequent recovery of subsamples during 5 d of irradiance of (**a**) *T. antarctica*, (**b**) *T. nordenskioeldii*, (**c**) *Micromonas* sp., and (**d**) *Rhodomonas* sp. The gray bars show the mean Chl *a* fluorescence after 5 d of recovery in an irradiance gradient (2–40 μmol photons m^{-2} s^{-1}, *n* = 10). For *T. nordenskioeldii*, recovery at 2 μmol photons m^{-2} s^{-1} is shown as white symbols.
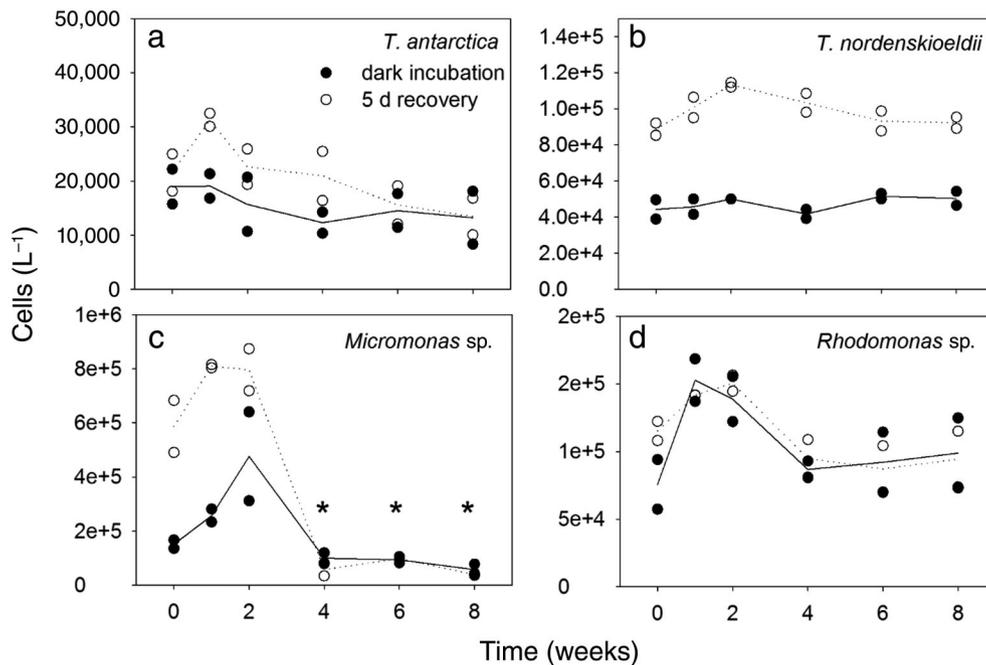
Fig. 3. Cell numbers during 8 weeks of dark incubation (black symbols) and subsequent recovery of subsamples during 5 d of irradiance (white symbols) of (**a**) *T. antarctica*, (**b**) *T. nordenskioeldii*, (**c**) *Micromonas* sp., and (**d**) *Rhodomonas* sp. The white symbols show the mean cell numbers after recovery in an irradiance gradient (2–40 μmol photons m^{-2} s^{-1}, *n* = 10). The stars indicate unreliable cell counts (*Micromonas* sp.) due to the pigment loss and the small size of this species.
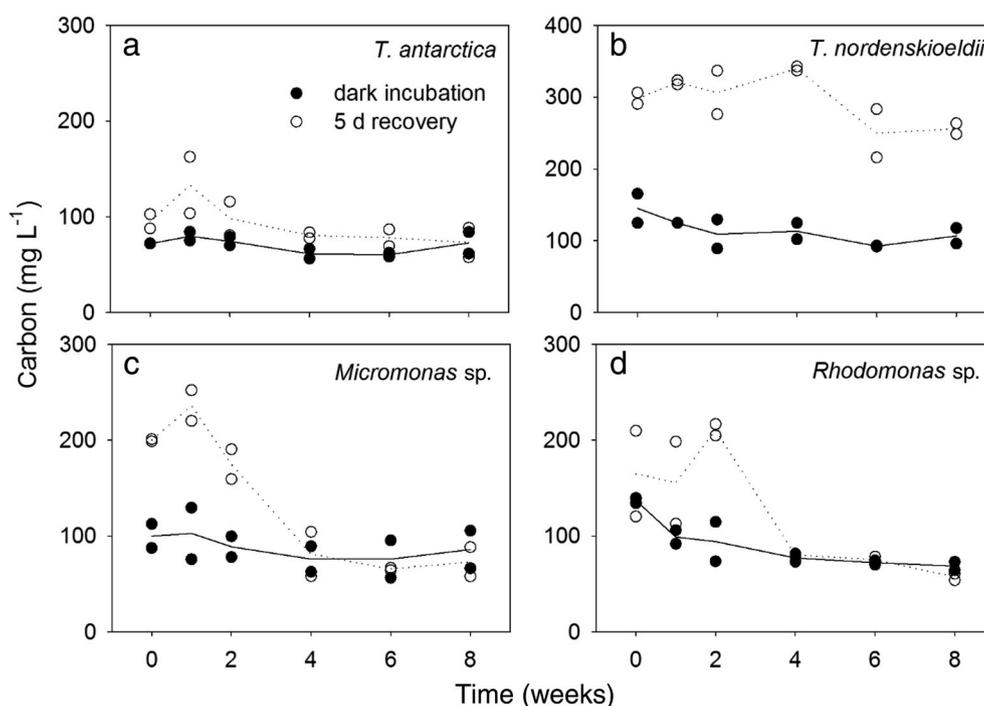
Fig. 4. Carbon during 8 weeks of dark incubation (black symbols) and subsequent recovery of subsamples during 5 d of irradiance (white symbols) of (**a**) *T. antarctica*, (**b**) *T. nordenskioeldii*, (**c**) *Micromonas* sp., and (**d**) *Rhodomonas* sp. The white symbols show the carbon concentration after 5 d of recovery under 20 μmol photons m^{-2} s^{-1}.

threefold (violaxanthin) and ninefold (zeaxanthin) increased ratios relative to Chl *a* (Table 3). For *Rhodomonas* sp., concentrations of Chl *a*, Chl c_2, alloxanthin, and β carotene during week 6 and 8 were on average 70% of the concentration during week 0, 1, 2, and 4. Ratios relative to Chl *a* were not significantly different during week 6, 8 as compared to week 0, 1, 2, 4 (Table 3).

Photosynthetic characteristics prior to dark incubation

Diatom maximum quantum yield of PSII during growth at 20 μmol photons m^{-2} s^{-1} was higher as compared to that of the flagellates (0.564 ± 0.005 vs. 0.515 ± 0.012). The absorption cross-section of PSII at 450 nm (σ_{PSII}[450]) of *Micromonas* sp. was higher when compared to the other species (9.1 vs. 3.8 nm^2 PSII^{-1}).

Moreover, PSII connectivity (ρ) was higher in *Micromonas* sp., whereas the reopening time of closed reaction center (τ_{ES}) was shorter as compared to the other species (not shown).

Photosynthetic characteristics during darkness

Maximum quantum yield of PSII (F_v/F_m) declined during darkness, with stronger decline rates observed for *Micromonas* sp. and *Rhodomonas* sp. as compared to the diatoms (Fig. 5, Table 1, $p = 0.029$). F_v/F_m decline rates were on average fivefold higher for flagellates as compared to those of diatoms. *Micromonas* sp. F_v/F_m became undetectable within 4 weeks, whereas this was 5 weeks for *Rhodomonas* sp. σ_{PSII}(450) declined in all species during dark incubation (Table 1). On average, the linear

Table 2. Pigments relative to Chl *a* of *T. antarctica* and *T. nordenskioeldii* during dark incubation. The mean of pooled samples is shown for the indicated time interval. dd + dt: diadinoxanthin and diatoxanthin pool. DES: de-epoxidation state of xanthophyll cycle. Mean carbon:Chl *a* ratios are shown for the same time interval. *p* values for significant differences between the dark incubation intervals are indicated in brackets.

Species	*T. antarctica*		*T. nordenskioeldii*	
Week	(0, 1, 2)	(4, 6, 8)	(0, 1, 2)	(4, 6, 8)
Chl c_2:Chl *a*	0.08	0.06	0.09	0.09
Fucoxanthin:Chl *a*	0.50	0.49	0.48	0.51 (< 0.001)
dd + dt:Chl *a*	0.05	0.06	0.05	0.06 (0.001)
β-carotene:Chl *a*	0.02	0.02	0.02	0.02
DES	0.24	0.36 (0.002)	0.16	0.43 (< 0.001)
Carbon:Chl *a*	90	105	39	36

Table 3. Pigments relative to Chl *a* of *Micromonas* sp. and *Rhodomonas* sp. during dark incubation. The mean of pooled samples is shown for the indicated time interval. In addition, mean carbon:Chl *a* ratios are shown for the same time interval. *p* values for significant differences between the dark incubation intervals are indicated in brackets.

Species	*Micromonas* sp.		*Rhodomonas* sp.	
Week	(0, 1, 2)	(4, 6, 8)	(0, 1, 2, 4)	(6, 8)
Mg-2,4-divinyl pheoporphyrin	0.05	0.05	—	—
Chl c_2:Chl *a*	—	—	0.14	0.14
Neoxanthin:Chl *a*	0.07	0.06 (< 0.001)	—	—
Prasinoxanthin:Chl *a*	0.23	0.26 (0.002)	—	—
Violaxanthin:Chl *a*	0.04	0.13 (0.002)	—	—
Antheraxanthin:Chl *a*	0.01	0.02	—	—
Zeaxanthin:Chl *a*	0.003	0.027 (< 0.001)	—	—
Alloxanthin:Chl *a*	—	—	0.29	0.28
Chl *b*:Chl *a*	0.66	0.71 (< 0.001)	—	—
β-carotene:Chl *a*	0.02	0.01	0.04	0.05
Carbon:Chl *a*	67	109 (< 0.001)	47	47

decline rates were 5.5-fold faster for flagellates as compared to diatoms ($p = 0.029$). PSII connectivity (ρ) of all species decreased during dark incubation, and decline rates were fivefold faster for flagellates as compared to diatoms ($p = 0.001$). Reopening time of closed RCII (τ_{ES} in μs) increased twofold faster for flagellates as compared to diatoms during dark incubation ($p = 0.029$). Stern-Volmer Normalized Stern-Volmer non-photochemical quenching (NPQ-NSV) increased in all species, the rate of increase was fivefold stronger in flagellates as compared to diatoms ($p = 0.009$).
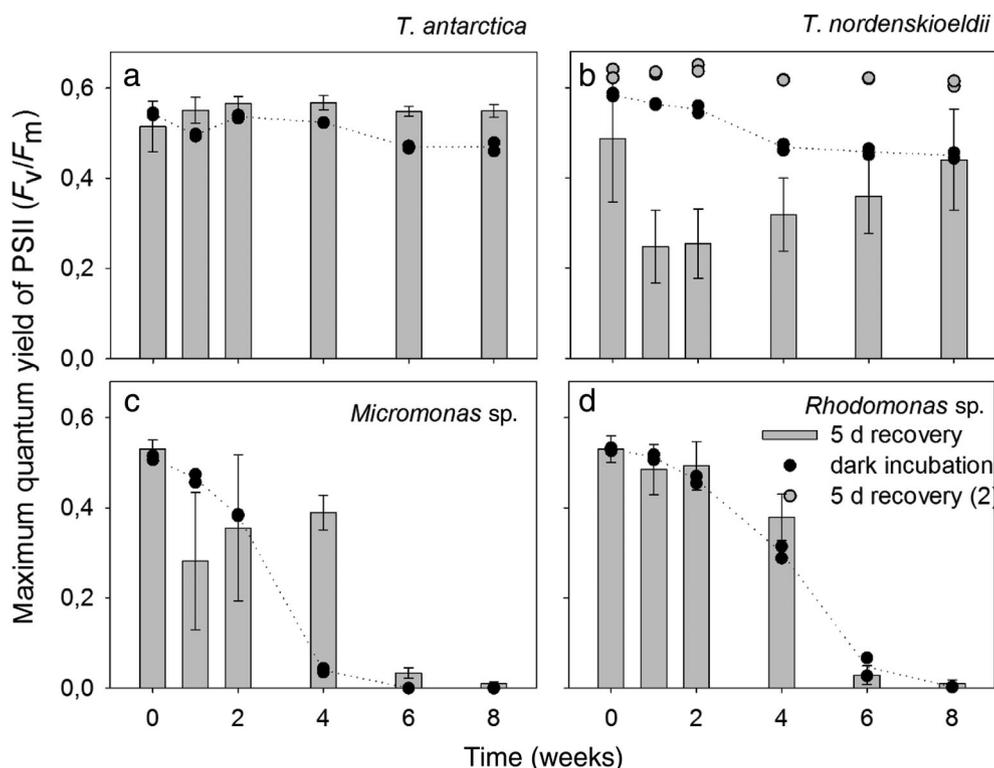
Fig. 5. Maximum quantum yield of PSII (FRRf) during 8 weeks of dark incubation and subsequent recovery of subsamples during 5 d of irradiance of (**a**) *T. antarctica*, (**b**) *T. nordenskioeldii*, (**c**) *Micromonas* sp., and (**d**) *Rhodomonas* sp. The gray bars show the mean and standard deviation of the maximum quantum yield of PSII after 5 d of recovery under an irradiance gradient (2–40 μmol photons m^{-2} s^{-1}, $n = 10$). For *T. nordenskioeldii*, recovery at 2 μmol photons m^{-2} s^{-1} is shown as gray circles.
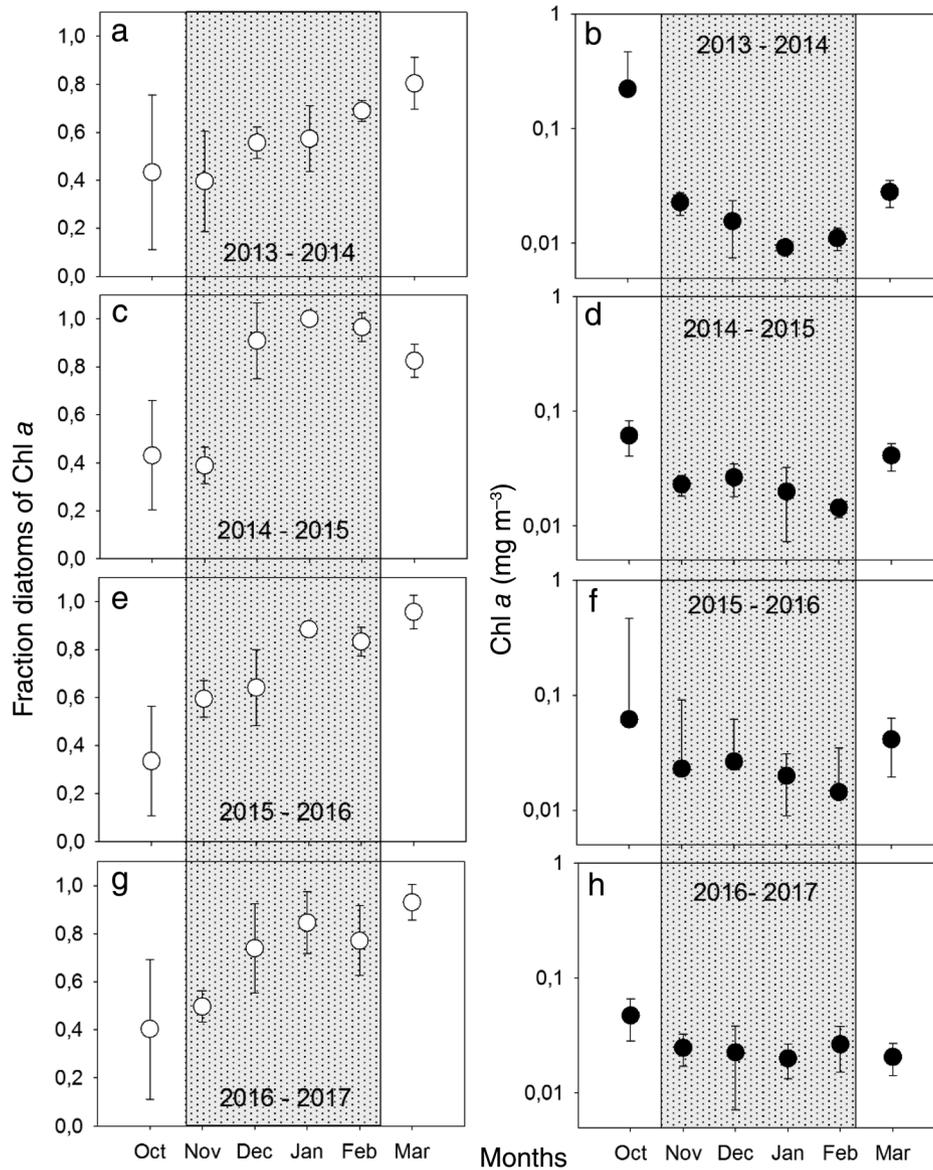
Fig. 6. Monthly mean fraction of diatoms (**a**, **c**, **e**, **g**) (white symbols, 0–1 scale) and monthly mean Chl *a* concentration (**b**, **d**, **f**, **h**) (black symbols) of pigment samples collected at the underwater Observatory in Kongsfjorden from October to March 2013–2017. The mean and standard deviation of four samples are shown. Chl *a* is presented on a logarithmic scale. The gray area indicates the polar night.

Recovery experiments after darkness (Chl *a*, cell numbers, and carbon)

When incubated for up to 2 weeks of darkness, 5 d of subsequent irradiance exposure during the recovery experiments resulted in 2–3-fold increased Chl *a* for all species, except for *Rhodomonas* sp., which showed a modest increase (120% of initial) during the recovery experiments (week 0, 1, 2, Fig. 1). No consistent patterns of irradiance specific differences were observed during the recovery experiments in the irradiance gradient (unless stated otherwise, i.e., *T. nordenskioeldii*). Instead, recovery responses of Chl *a* and photosynthetic activity depended on the duration of dark incubation. Therefore,

the data of the five irradiance levels were pooled. Accumulated Chl *a* during the recovery experiments declined after longer dark incubation (recovery experiments week 4, 6, 8) except for *T. nordenskioeldii*, which showed consistently 2.7-fold increased Chl *a* after recovery. *T. antarctica* Chl *a* after recovery was on average 126% of the initial concentration during experiments after 4–8 weeks dark incubation. Chl *a* of *Rhodomonas* sp. and *Micromonas* sp. declined during 5 d of recovery after 4–8 weeks of dark incubation to 50% and 16% of initial concentration, respectively. Chl *a* after recovery of these species showed a negative correlation with irradiance ($R^2 = 0.9$, results not shown) when dark incubated in excess of 2 weeks. Patterns

of FRRf derived Chl *a* fluorescence (F0) were highly similar to those of fluorometrically determined Chl *a* (Fig. 2).

Cell numbers of *T. antarctica*, *T. nordenskioeldii*, and *Micromonas* sp. increased during the 5 d recovery treatment of dark incubated samples (week 0, 1, 2) as compared to cell numbers recorded directly after dark incubation (Fig. 3). For *Rhodomonas* sp., increased Chl *a* after 5 d recovery did not coincide with increased cell numbers. Positive growth rates during recovery were not observed for *Micromonas* sp., *Rhodomonas* sp., and *T. antarctica* after 2 weeks of dark incubation (recovery experiments week 4, 6, 8). *T. nordenskioeldii* maintained positive recovery growth rates during 8 weeks of dark incubation (Fig. 3).

POC concentrations after 5 d of recovery at 20 μmol photons m^{-2} s^{-1} of all species increased during the initial 2 weeks of dark incubation (Fig. 4). Dark incubation longer than 2 weeks showed no increased POC after recovery experiments of *Micromonas* sp. and *Rhodomonas* sp. *T. nordenskioeldii* accumulated POC during recovery experiments throughout 8 weeks of dark incubation.

Photosynthetic characteristics during recovery experiments

Maximum quantum yield of PSII (F_v/F_m) after 5 d of recovery in irradiance was higher (*T. antarctica*), similar (*Rhodomonas* sp.), or lower (*T. nordenkioeldii*, *Micromonas* sp.) as compared to directly after dark incubation (Fig. 5). Low F_v/F_m compared to the dark incubation values corresponded to increased Chl *a* after 5 d of recovery (i.e., *T. nordenskioeldii* [week 0–8], *Micromonas* sp. [week 0–2]), which we attributed to nutrient limitation. F_v/F_m of phosphate- and/or nitrate-limited cultures is known to decrease (Van de Poll et al. 2005). Due to potential nutrient limitation and the variability in accumulated biomass during the 5 d recovery experiments, a meaningful comparison of photophysiological characteristics with dark incubated samples was not possible. F_v/F_m of *Micromonas* sp. increased nearly 10-fold during the recovery experiment after 4 weeks of dark incubation (average 0.04–0.4). This coincided with strongly reduced Chl *a*. We explained this result as the recovery of a limited number of viable cells.

Kongsfjorden pigment monitoring during the polar night

Downwelling irradiance in Ny Ålesund (as measured in 2013 by the Baseline Surface Radiation Network [BSRN] pyranometer of the AWIPEV station) showed strong seasonality, in October 72.5% of hourly averaged PAR was below 0.5 μmol photons m^{-2} s^{-1} with a maximal irradiance of 25 μmol photons m^{-2} s^{-1}. During November, December, and January, hourly averaged PAR was below 1 μmol photons m^{-2} s^{-1} and 99.1% of this was below 0.5 μmol photons m^{-2} s^{-1}. Sunlight increased by the end of February (with 87.5% of hourly averaged PAR still below 0.5 μmol photons m^{-2} s^{-1}). During March and April, 52.5% and 93% of hourly averaged irradiance was above 0.5 μmol photons m^{-2} s^{-1}, respectively (Maturilli et al. 2019; Pavlov et al. 2019).

Chl *a* declined 10-fold from October (average 2013–2016: 0.29 mg m^{-3}) to a minimum in January/February (average 2013–2017: 0.02 mg m^{-3}) (Fig. 6). Spearman rank correlation coefficients showed significantly declining Chl *a* from October to February during all years. Increasing irradiance in March coincided with slightly increased Chl *a* (average March 2013–2017: 0.03 mg m^{-3}). Due to low biomass concentrations during the polar night, not all marker pigments were above the detection limit. Fucoxanthin was detected in all samples ($n = 96$), Chl *b* was not detected in 25 samples, 19-hexanoloxyfucoxanthin was not detected in 32 samples, alloxanthin was absent in 56 samples, and peridinin was detected in only 12 samples. Because this resulted in variability in CHEMTAX output, we averaged monthly values for each year with respect to CHEMTAX derived taxonomic composition. On average, October to March samples (2013–2017) consisted of 67% ± 25% diatoms; 22% ± 21% haptophytes, and 9% ± 8% prasinophytes, whereas cryptophytes comprised 2.2% of Chl *a*. Samples from October to March were rich in fucoxanthin (average ratio fucoxanthin relative to Chl *a* from October to February: 0.32 ± 0.07; March: 0.42 ± 0.1). Taxonomic composition as determined by CHEMTAX showed an increasing contribution of diatoms from October (40% ± 5% diatoms) to March (88% ± 8% diatoms) (Fig. 6). Spearman rank correlation coefficients showed significantly increasing contributions of diatoms to Chl *a* from October to March for all years.

Discussion

Our experiments underline the fundamental differences in responses of diatoms and flagellates to prolonged darkness. Diatoms survive longer than flagellates when exposed darkness on a time scale that is relevant during winter in large parts of the Arctic. These differences might be due to differences in the allocation of energy reserves, with diatoms utilizing a more conservative approach as compared to flagellates, resulting in prolonged survival of long periods of darkness, while maintaining the ability to photosynthesize when returned to irradiance (Walter et al. 2017). Diatoms may have evolved these survival mechanisms as an adaptation to seasonal variability in irradiance and macronutrient (nitrate, phosphate, silicic acid) concentrations. Diatoms are also known to possess a dissimilatory nitrate reduction to ammonium activity that might provide energy during times of low irradiance (Kamp et al. 2011). However, this is not believed to sustain metabolism during long-term survival of diatoms under dark conditions. In contrast, the flagellates allocated stored energy to cell division and photoacclimation during darkness, traits which can be advantageous when nutrient concentrations are low. The taxon-specific survival traits observed during the dark incubation experiments suggest that periods of prolonged darkness such as the polar night can influence phytoplankton composition, that is, the geographic distribution and phenology of flagellates and diatoms. This

was confirmed for Kongsfjorden (Spitsbergen), a mostly ice free fjord in the high Arctic that experiences a 116 d polar night. The changes in relative phytoplankton composition in favor of diatoms during the polar night coincided with declining Chl *a* for all 4 yr of observation. Without irradiance for growth, loss factors such as grazing also contribute to the decline in Chl *a* (Berge et al. 2015). However, our experiments provide evidence that this may also be due to taxon-specific decline rates in cellular Chl *a* and due to taxon-specific mortality of groups with less survival potential during long periods of darkness. Therefore, the ability to survive periods of darkness can cause a relative enrichment of diatoms at latitudes that experience darkness in excess of 4 weeks. Traditionally, the occurrence diatoms and their presence during spring blooms has been attributed to their high growth rates and capacity to compete at low irradiance. This is also how diatoms are represented in biogeochemical models such as PISCES-NEMO (Aumont et al. 2015) and REcoM2 (Schourup-Kristensen et al. 2018). However, these assumptions are not univocally supported by field and lab observations. Under nutrient replete conditions, reported growth rates of diatoms are in the same range as those reported for other eukaryotic phytoplankton (Gilstad and Sakshaug 1990; Hoppe et al. 2018). Furthermore, the Antarctic haptophyte *P. antarctica* showed a stronger productivity in low irradiance as compared to the diatom *Fragillariopsis* sp. (Arrigo et al. 2010). The specific growth rates of the diatom species investigated in this study are also not higher than those of the flagellates, although differences in photosynthetic characteristics between *Micromonas* and the larger diatom and cryptophyte species were evident. Although far from exhaustive, this suggests that the scientific base for higher maximal productivity rates of diatoms is weak. Instead, we suggest that other mechanisms may be responsible for the early occurrence of diatoms during high latitude spring blooms, such as their ability to survive prolonged periods of darkness. Not only do diatoms survive long periods of darkness, they also maintain the ability to commence growth within 5 d upon exposure to irradiance as observed during the recovery experiments. Elongated dark survival enables diatoms to exploit the high nutrient stocks in early spring when the irradiance returns.

At our pigment monitoring site, other structural observations of phytoplankton composition during the polar night are lacking. Apart from diatoms, also photosynthetic genes of *Micromonas* sp. and other photosynthetic flagellates can be found during the polar night on the west coast of Spitsbergen (Vader et al. 2014; Marquardt et al. 2016). The combination of Arctic and Atlantic influences presumably has a strong influence on Kongsfjorden phytoplankton composition. Atlantic water masses of the West Spitsbergen Current may carry viable flagellate populations into Kongsfjorden. Therefore, lateral advection of phytoplankton with different irradiance history can also influence taxonomic composition at this site. Final stages of the spring bloom in Kongsfjorden (maximal Chl *a*

concentrations 10 μg L^{-1}, in the proximity of the surface) are typically observed in May and June after stratification of the water column (Hegseth and Tverberg 2013; Van de Poll et al. 2016). These stages are not consistently dominated by diatoms (Hegseth and Tverberg 2013; Van de Poll et al. 2016, 2018; Hegseth et al. 2019). This suggests that the competitive advantage of diatoms in early spring does not necessarily imply that this group dominates the final stages of the spring bloom. Two months is a long time for organisms with a turn-over time in the order of several days. Furthermore, elongated irradiance exposure (up to 24 h per day) in April facilitates the proliferation of species that do not possess strong survival capabilities. This shows that spring time phytoplankton composition in Kongsfjorden also depends on other mechanism than dark survival alone such as lateral advection of phytoplankton populations with a different irradiance history. Dark survival of the haptophyte *Phaeocystis pouchetii*, an important species during high latitude spring and summertime blooms, has not been investigated so far. Mixotrophy has been observed in flagellates such as *Micromonas pusilla* and *Rhodomonas* sp., for the former ingestion rates of bacteria appeared to be irradiance dependent, making it unlikely that this process could replace photosynthesis as a mechanism to generate energy during the polar night (McKie-Krisberg and Sanders 2014). Moreover, abundance of prey organisms such as bacteria and small flagellates is much lower during the polar night, reducing encounter rates. However, heterotrophic dinoflagellates are present during the polar night in Kongsfjorden, demonstrating that this life style can be maintained during prolonged darkness (Seuthe et al. 2011; Berge et al. 2015; Kvernvik et al. 2018).

Cultures of all examined species remained viable during 2 weeks of darkness. Flagellates showed stronger responses as compared to the diatoms during the initial 2 weeks of darkness, which resulted in increased Chl *a* and cell numbers in the absence of irradiance. This was despite a decline in photosynthetic characteristics that occurred within this time interval at the light harvesting/photosystem II level. The rates of degradation were species specific, with the diatoms showing lower degradation rates as compared to the flagellates. Furthermore, flagellates lost FRRf based photosynthetic characteristics and the ability to recover during 5 d of irradiance within 4–6 weeks, demonstrating that long dark incubation resulted in irreversible degradation of the photosynthetic machinery, ranging from pigments to membrane components and enzymes. This contrasted with the diatom *T. nordenskioeldii* that maintained photosynthetic characteristics and a strong recovery potential over 8 weeks of darkness. *T. antarctica* showed a reduced potential for growth after 2 weeks, while showing similar photosynthetic characteristics during darkness as *T. nordenskioeldii*. Both diatoms cultures were able to grow after 8 weeks of dark incubation when returned to the original irradiance. Nevertheless, this suggested variability in recovery responses within the diatom genus, as were also observed between *Micromonas* sp. and *Rhodomonas* sp. Pigment composition changed as a result of prolonged dark incubation, although

changes relative to Chl *a* were modest (~ 20% change during 8 weeks of dark incubation) compared to the strong taxon-specific changes in pigment concentrations. Therefore, these changes have a limited potential to bias pigment-based taxonomic composition estimates (CHEMTAX) during the polar night. Strongest fluctuations were observed in xanthophyll cycle pigments (diadino, diatoxanthin, viola, zeaxanthin). Increased diatoxanthin (diatoms) and zeaxanthin (*Micromonas* sp.) relative to Chl *a* can be explained as measure to increase nonphotochemical quenching capacity in response to reduced photosynthetic capacity. Although accessory pigments changes relative to Chl *a* varied in a narrow range, carbon to Chl *a* changed up to a factor 2. Moreover, pigments and carbon of nonviable *Micromonas* sp. and *Rhodomonas* sp. cultures persisted in excess of 4 weeks in darkness, of which the former degraded upon irradiance exposure. This suggests that a fraction of Chl *a* and carbon during the polar night can belong to non-viable phytoplankton, and as such can make carbon and Chl *a* unreliable estimators of phytoplankton biomass during the polar night.

Our experiments do not exactly mimic the changes in irradiance and day length experienced prior and after the polar night (Maturilli et al. 2019; Pavlov et al. 2019), nor do they cover all key species involved in phytoplankton bloom formation. Nevertheless, both experimental and field observations suggest that differences in long-term dark survival between diatoms and flagellates can play a role in explaining their presence during high latitude spring blooms after experiencing a polar night. These traits have potential influence on the geographical distribution into high latitude regions of diatoms and flagellates, with diatoms having an advantage in regions with prolonged absence of irradiance.

References

Arrigo, K. R., M. M. Mills, L. R. Kropuenske, G. L. van Dijken, A. C. Alderkamp, and D. H. Robinson. 2010. Photophysiology in two major southern ocean phytoplankton taxa: Photosynthesis and growth of *Phaeocystis antarctica* and *Fragilariopsis cylindrus* under different irradiance levels. Integr. Comp. Biol. **50**: 950–966. doi:10.1093/icb/icq021

Aumont, O., C. Ethé, A. Tagliabue, L. Bopp, and M. Gehlen. 2015. PISCES-v2: An ocean biogeochemical model for carbon and ecosystem studies. Geosci. Model Dev. **8**: 2465–2513. doi:10.5194/gmd-8-2465-2015

Berge, J., et al. 2015. Unexpected levels of biological activity during the polar night offer new perspectives on a warming Arctic. Curr. Biol. **25**: 2555–2561. doi:10.1016/j.cub.2015.08.024

Fischer, P., M. Schwanitz, R. Loth, U. Posner, M. Brand, and F. Schröder. 2017. First year of practical experiences of the new Arctic AWIPEV-COSYNA cabled Underwater Observatory in Kongsfjorden, Spitsbergen. Ocean Sci. **13**: 259–272. doi:10.5194/os-13-259-2017

Gilstad, M., and E. Sakshaug. 1990. Growth rates of ten diatom species from the Barents Sea at different irradiances and day lengths. Mar. Ecol. Prog. Ser. **64**: 169–173.

Guillard, R. R. L., and J. H. Ryther. 1962. Studies of marine planktonic diatoms: I. *Cyclothella nana* Hustedt, and *Detonula confervacea* (Cleve) gran. Can. J. Microbiol. **8**: 229–239.

Hegseth, E. N., and V. Tverberg. 2013. Effect of Atlantic water inflow on timing of the phytoplankton spring bloom in a high Arctic fjord (Kongsfjorden, Svalbard). J. Mar. Syst. **113–114**: 94–105. doi:10.1016/j.jmarsys.2013.01.003

Hegseth, E. N., et al. 2019. Phytoplankton seasonal dynamics in Kongsfjorden, Svalbard and the adjacent shelf. p. 173–227. *In* H. Hop and C. Wiencke [eds.], The ecosystem of Kongsfjorden, Svalbard. Advances in polar ecology, v. **2**. Springer.

Hoppe, C. J. M., C. M. Flintrop, and B. Rost. 2018. The Arctic picoeukaryote *Micromonas pusilla* benefits synergistically from warming and ocean acidification. Biogeosciences **15**: 4353–4365. doi:10.5194/bg-15-4353-2018

Joli, N., A. Monier, R. Logares, and C. Lovejoy. 2017. Seasonal patterns in Arctic prasinophytes and inferred ecology of *Bathycoccus* unveiled in an Arctic winter metagenome. ISME J. **11**: 1372–1385. doi:10.1038/ismej.2017.7

Kamp, A., D. de Beer, J. L. Nitsch, G. Lavik, and P. Stief. 2011. Diatoms respire nitrate to survive dark and anoxic conditions. Proc. Natl. Acad. Sci. USA **108**: 5649–5654. doi:10.1073/pnas.1015744108

Kolber, Z. S., O. Prasil, and P. G. Falkowski. 1998. Measurements of variable chlorophyll fluorescence using fast repetition rate techniques: Defining methodology and experimental protocols. Biochim. Biophys. Acta **1367**: 88–106.

Kvernvik, A. C., C. J. M. Hoppe, E. Lawrenz, O. Prášil, M. Greenacre, J. M. Wiktor, and E. Leu. 2018. Fast reactivation of photosynthesis in arctic phytoplankton during the polar night. J. Phycol. **54**: 461–470. doi:10.1111/jpy.12750

Lewis, J., A. S. D. Harris, K. J. Jones, and R. L. Edmonds. 1999. Long-term survival of marine planktonic diatoms and dinoflagellates in stored sediment samples. J. Plankton Res. **21**: 343–354.

Mackey, M. D., H. W. Higgins, D. J. Mackey, and S. W. Wright. 1996. CHEMTAX – a program for estimating class abundances from chemical markers: Application to HPLC measurements of phytoplankton. Mar. Ecol. Prog. Ser. **144**: 265–283. doi:10.3354/meps144265

Marquardt, M., A. Vader, E. I. Stübner, M. Reigstad, and T. M. Gabrielsen. 2016. Strong seasonality of marine microbial eukaryotes in a high-Arctic fjord (Isfjorden, in West Spitsbergen, Norway). Appl. Environ. Microbiol. **82**: 1868–1880. doi:10.1128/AEM.03208-15

Maturilli, M., I. Hanssen-Bauer, R. Neuber, M. Rex, and K. Edvardsen. 2019. The atmosphere above Ny-Ålesund: Climate and global warming, ozone and surface UV radiation. *In* H. Hop and C. Wiencke [eds.], The ecosystem of

Kongsfjorden, Svalbard. Advances in polar ecology, v. **2**. Springer.

McKie-Krisberg, Z., and R. W. Sanders. 2014. Phagotrophy by the picoeukaryotic green alga *Micromonas*: Implications for Arctic oceans. ISME J. **8**: 1953–1961. doi:10.1038/ismej.2014.16

McMinn, A., and A. Martin. 2013. Dark survival in a warming world. Proc. Biol. Sci. **280**: 20122909. doi:10.1098/rspb.2012.2909

Pavlov, A. K., et al. 2019. The underwater light climate in Kongsfjorden and its ecological implications. p. 137–170. *In* H. Hop and C. Wiencke [eds.], The ecosystem of Kongsfjorden, Svalbard. Advances in polar ecology, v. **2**. Springer.

Peters, E., and D. N. Thomas. 1996. Prolonged darkness and diatom mortality I: Marine Antarctic species. J. Exp. Mar. Biol. Ecol. **207**: 25–41.

Reeves, S., A. McMinn, and A. Martin. 2011. The effect of prolonged darkness on the growth, recovery and survival of Antarctic Sea ice diatoms. Polar Biol. **34**: 1019–1032.

Schaub, I., H. Wagner, M. Graeve, and U. Karsten. 2017. Effects of prolonged darkness and temperature on the lipid metabolism in the benthic diatom *Navicula perminuta* from the Arctic Adventfjorden, Svalbard. Polar Biol. **40**: 1425–1439. doi:10.1007/s00300-016-2067-y

Schourup-Kristensen, V., C. Wekerle, D. A. Wolf-Gladrow, and C. Völker. 2018. Arctic Ocean biogeochemistry in the high resolution FESOM 1.4-REcoM2 model. Prog. Oceanogr. **168**: 65–81. doi:10.1016/j.pocean.2018.09.006

Seuthe, L., K. R. Iversen, and F. Narcy. 2011. Microbial processes in a high-latitude fjord (Kongsfjorden, Svalbard): II. Ciliates and dinoflagellates. Polar Biol. **34**: 751–776. doi:10.1007/s00300-010-0930-9

Stoecker, D. K., and P. J. Lavrentyev. 2018. Mixotrophic plankton in the polar seas: A pan-Arctic review front. Mar. Sci. **22**: 1–12. doi:10.3389/fmars.2018.00292

Tang, K. W., W. O. Smith Jr., A. R. Shields, and D. T. Elliott. 2009. Survival and recovery of *Phaeocystis antarctica* (Prymnesiophyceae) from prolonged darkness and freezing. Proc. Biol. Sci. **276**: 81–90. doi:10.1098/rspb.2008.0598

Vader, A., M. Marquardt, A. Meshram, and T. M. Gabrielsen. 2014. Key Arctic phototrophs are widespread in the polar night. Polar Biol. **38**: 13–21. doi:10.1007/s00300-014-1570-2

Van de Poll, W. H., M. van Leeuwe, J. Roggeveld, and A. G. J. Buma. 2005. Nutrient limitation and high irradiance reduce PAR and UV-induced viability loss in the Antarctic diatom *Chaetoceros brevis*. J. Phycol. **41**: 840–850.

Van de Poll, W. H., D. S. Maat, P. Fischer, P. D. Rozema, O. B. Daly, S. Koppelle, R. J. W. Visser, and A. G. J. Buma. 2016. Atlantic advection driven changes in glacial meltwater: Effects on phytoplankton chlorophyll a and taxonomic composition in Kongsfjorden, Spitsbergen. Front. Mar. Sci. **3**: 1–11. doi:10.3389/fmars.2016.00200

Van de Poll, W. H., G. Kulk, P. D. Rozema, C. P. D. Brussaard, R. J. W. Visser, and A. G. J. Buma. 2018. Contrasting glacial meltwater effects on post-bloom phytoplankton on temporal and spatial scales in Kongsfjorden, Spitsbergen. Elem. Sci. Anth. **6**: 50. doi:10.1525/elementa.307

Van Heukelem, L., and C. S. Thomas. 2001. Computer-assisted high-performance liquid chromatography method development with applications to the isolation and analysis of phytoplankton pigments. J. Chromatogr. A **910**: 31–49. doi:10.1016/S0378-4347(00)00603-4

Van Leeuwe, M. A., L. A. Villerius, J. Roggeveld, R. J. W. Visser, and J. Stefels. 2006. An optimized method for automated analysis of algal pigments by HPLC. Mar. Chem. **102**: 267–275. doi:10.1016/j.marchem.2006.05.003

Veuger, B., and D. van Oevelen. 2011. Long-term pigment dynamics and diatom survival in dark sediment. Limnol. Oceanogr. **56**: 1065–1074. doi:10.4319/lo.2011.56.3.1065

Walter, B., J. Peters, and J. E. E. van Beusekom. 2017. The effect of constant darkness and short light periods on the survival and physiological fitness of two phytoplankton species and their growth potential after re-illumination. Aquat. Ecol. **51**: 591–603. doi:10.1007/s10452-017-9638-z

Wassmann, P., T. Ratkova, I. Andreassen, M. Vernet, G. Pedersen, and F. Rey. 1999. Spring bloom development in the marginal ice zone and the central Barents Sea. Mar. Ecol. **20**: 321–346.

Conflict of Interest

None declared.